

Research Article

First-Principles Investigation of structural, Optical, and Electrical properties of MgO Nanocrystals

Received 9th April 2021
 Revised 17th July 2021
 Accepted 25th July 2021

DOI:
<https://doi.org/10.22452/mnij.vol1no1.2>

Corresponding author:
 drsureshnano@gmail.com

Nur 'Adnin Akmar Zulkifli^a, Rozalina Zakaria^a, Suresh Sagadevan^{b*}, A.R. Marlinda^b, Nor Aliya Hamizi^b and Mohd Rafie Johan^b

^aPhotonics Research Centre, Faculty Science, University of Malaya, 50603, Kuala Lumpur, Malaysia

^bNanotechnology and Catalysis Research Centre, University of Malaya, 50603, Kuala Lumpur, Malaysia

Abstract

Nanocrystal interfaces can strongly influence the optical and electrical properties and charging trapping phenomena observed on oxide nanocrystal ensembles. The well-defined shape and controllable size distributions of MgO nanocrystals are a convenient system for studying these effects. Therefore, in the present work focused on the effect of temperature on the optical and electrical properties of magnesium oxide (MgO) nanocrystals, together with the responsible atomic centers, the bulk MgO is a study based on the first principle functional density theory (DFT) using PBE-GGA approximations. The absorption coefficient shows that MgO shows good coverage in the ultraviolet range. The bulk MgO is a direct bandgap nanocrystal at G point in the Brillion Zone despite the temperature applied values. The temperature is applied to alter the bandgap pattern and closes the bandgap at a high temperature. The PDOS and imaginary part of the dielectric function further confirm the insulator properties of the observed bandgap. Our results show that the optical properties are affected by the inconsistent temperature manners despite the different temperatures given to the system. Our absorption curve confirms that the nanocrystal is a good candidate for ultraviolet device application with a significantly high reflectivity percentage.

Keywords: DFT, MgO nanocrystals, Optical and electrical properties

1. Introduction

Metal oxides are basic functional materials with a wide range of chemical, physical and material science applications [1]. They are generally used for photocatalytic purposes [2], biomedical engineering [3], and sensors [4-6] due to their easy and controllable synthesis. The size and surface morphology of metal oxides depends on the route of synthesis, pH, temperature, and time of annealing [7] and can, therefore, be controlled during the process of growth. Magnesium oxide (MgO), a wide-bandgap insulator, has promising electronics applications due to its intriguing features such as low cost, non-toxicity, high-temperature resistance, optical transmittance, and rich earthly abundance. Due to their unique and often tunable properties, metal oxide nanocrystals powders find important applications [8,9]. Much research has focused on such nanopowders on understanding photoexcited processes. Compared to bulk materials, nanoparticles have different properties. Most researchers work with metal oxide nanoparticles due to their unique characteristics such as hydrophobic, photocatalytic, and stability [10]. Because of its large bandgap and cheap manufacturing, researchers worldwide have been attracted by MgO nanoparticles. MgO has a large bandgap (~ 7 eV) and is an insulator. Responsible for their increased reactivity is a reduced bandgap of MgO nanoparticles [11]. Numerous theoretical and experimental investigations on MgO nanocrystals have been carried out to date. One valuable method for calculating the molecules' optical and electronic properties is using solid-state density functional theory (DFT)[12,13]. Calculations of the first principles using Local Density Approximation (LDA) or Generalized Gradient Approximation (GGA) [14] are few methods of calculating electronic and optical properties. Although in the case of transition metal oxides, these methods lead to significant underestimation of the bandgap. The GGA functional is often considered reliable. It does not alter the bandgap pattern of a structure [15].

This study used the first principle functional density theory (DFT) to perform a detailed calculation of effect temperature on MgO nanocrystal's electronic and optical properties. The structural parameters were changed under temperature, including constant lattice and bond length, directly affecting the electronic structure and optical characteristics.

2. Computational Methods

We performed our calculations using the Total Energy Package (CASTEP) provided by Material studio based on the first principle density functional theory (DFT). The MgO nanoparticle has a G 225 (Fm-3m) space group and similarity in structure as the NaCl cubic with $a=b=c$. The ultra-soft pseudopotential was adopted to describe the ion-electron interaction using the generalized gradient approximation (GGA) with the Perdew-Burke- Ernzerhof (PBE) functional. The geometry optimization and electrical properties were performed with the energy cut-off 380 eV and Monkhorst-Pack k point mesh of $4 \times 4 \times 4$ in the Brillouin zone sampling. The convergence energy displaces, and forces were set at 5×10^{-6} eV/atom, 5×10^{-4} Å, and 0.01 eV/Å, respectively. To investigate the optical properties, we performed our calculations on the same optimized structure using the norm-conserving pseudopotentials with the cut-off energy of 900 eV and the same k-point grid of $4 \times 4 \times 4$. Observation of temperature that influences the MgO structure, the different thermal conditions (T=100 K, 300 K, 600 K) are also considered, and the effect on the electrical and optical properties is analyzed. The molecular dynamic module is employed to gain accurate data.

3. Results and Discussion

3.1. Structural Properties

To obtain a stable structure, the finest geometry optimization of MgO nanocrystal was first performed on the unit cell basis as shown in Figure 1 using the established crystallographic data provided by Wyckoff et al. [16] lattice parameter $a_0 = 4.216$ Å. Then, the MgO nanocrystal was fully relaxed to $a_0 = 4.299$ Å, and the bond length of Mg – Mg, and Mg – O are 3.040 Å and 2.150 Å, respectively. To investigate the MgO nanocrystal temperature dependency on the electrical and optical properties, we also consider running out three different thermal conditions of T = 100K, 300K, and 600 and employ the molecular dynamic to achieve accurate data. To see the effect of our structure's temperature, we also consider plotting the lattice parameter MgO graph at different temperatures (Figure 2). As expected, results show a non-linear direct proportional relationship between the lattice parameter and temperature due to the thermal expansion [17].

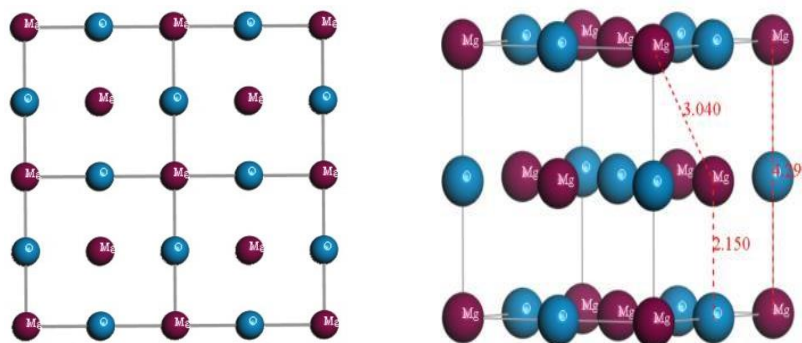


Figure 1: Top view of 2 x 2 x 1 supercell MgO. The grey line indicates one unit cell. (left), and side view of DFT optimized unit cell structure MgO nanocrystal having Fm-3m crystal symmetry.

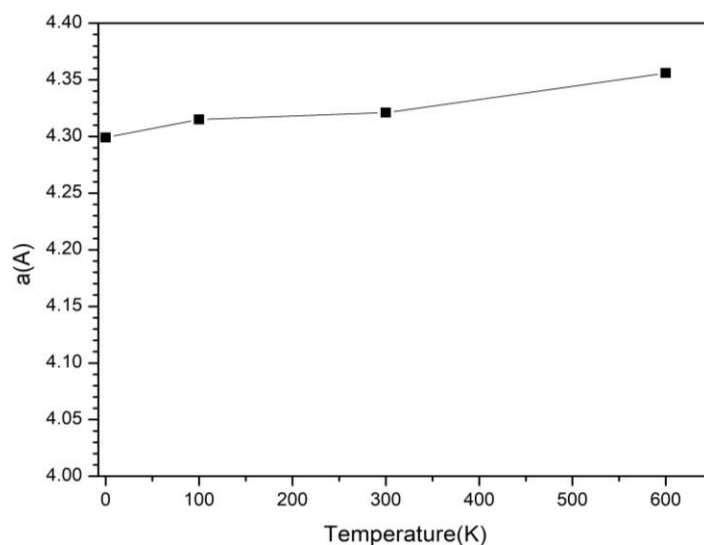


Figure 2; The variation of lattice parameter (Å) with temperature (K)

3.2 Optical Properties

Figure 3 represents the optical properties for this nanocrystal-based dielectric function, absorption coefficient $\alpha(\omega)$, loss function $L(\omega)$, and reflectivity $R(\omega)$ for parallel field polarization ($E||x$) to the MgO structure. From the joint density of states and momentum matrix element, the imaginary part $\epsilon_2(\omega)$ of the dielectric function is obtained. Then, by applying the Kramer-Kronig transformations, the real part $\epsilon_1(\omega)$ is then derived from the $\epsilon_2(\omega)$. The complex dielectric function is expressed in real and imaginary parts by the following equation,

$$\varepsilon(\omega) = \varepsilon_1 + \varepsilon_2 \quad (1)$$

where ε_1 and ε_2 is real (dispersive) and imaginary (absorptive) part of the function, respectively. The static dielectric constant (ε_0) and bandgap value E_g are inversely proportional related by the Penn Model of the equation.

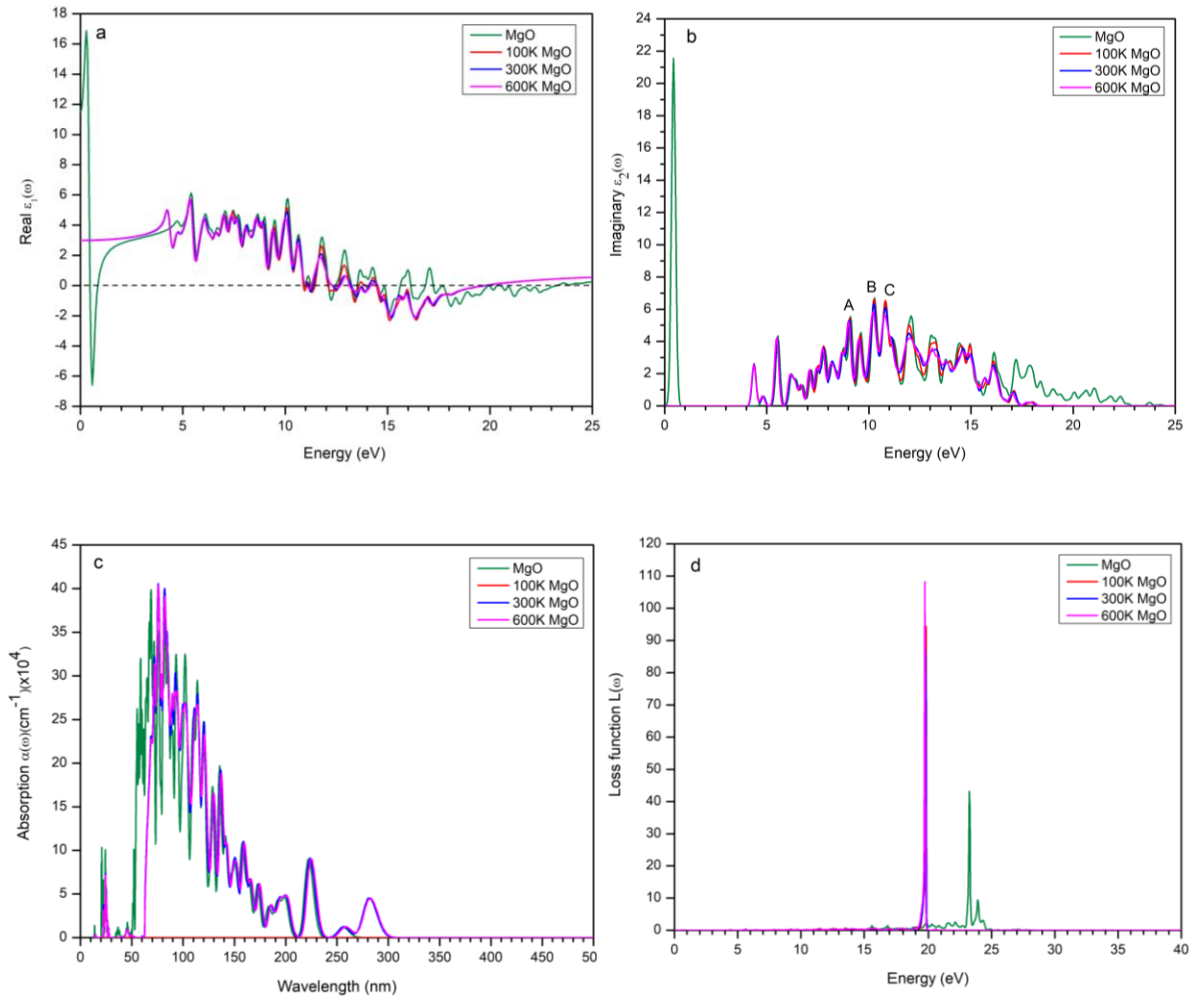
$$\varepsilon \approx 1 + (\hbar\omega_p/E_g)^2 \quad (2)$$

As seen in Figure 3(a), the real part $\varepsilon_1(\omega)$ of the dielectric function, the static dielectric constant of MgO within the zero-frequency limit without thermal effect, is observed considerably high of 11.5 eV. For the 100K, 300K, and 600K temperature effect, the ε_0 value was observed at 3.0 eV. We also note a sharp negative profile at 0.7 eV and 10.8 to 23.4 eV without thermal effect. From 10.9 to 19.8 eV for all three-temperature applied, the MgO nanocrystal shows metallic behaviour in these zones of frequency. The imaginary part of the dielectric function is presented in Fig. 3(b). We observe a gap between 0 eV to 4.1 eV, where this gap is independent of the incident light's direction. After 4.1 eV, a very sharp increase occurs, and these peaks indicate the first transition from the valence to the conduction band of this compound. The threshold energy for MgO, 100K MgO, 300K MgO, and 600 MgO obtained from the imaginary part is 4.180 eV, 4.071 eV, and 4.076 eV 3.876 eV, respectively to the fundamental absorption edge at equilibrium. There are three significant peaks identified from profile A (5.6 at 9.0 eV), B (6.8 at 10.2 eV), and C (6.6 at 10.9 eV). When the intensity of the photons increases, the amount of the transition decreases gradually. Most of these transitions occur from the orbitals 3p Mg orbital to the 2p Oxygen orbital. The transition stops at 24.5 eV and 18.5 eV when the temperature is given. We also analyze the optical properties through the absorption coefficient. This graph tells the photon energies that are most likely to be absorbed by the structures and benefit in designing a suitable device application. The absorption coefficient is expressed in terms of $\varepsilon_1(\omega)$ and $\varepsilon_2(\omega)$ by the following equation,

$$\alpha(\omega) = \frac{\sqrt{2\omega}}{c} \{[\varepsilon_1^2(\omega) + \varepsilon_2^2(\omega)]^{\frac{1}{2}} - \varepsilon_1(\omega)\} \quad (3)$$

Figure 3(c) shows the capacity of MgO to absorb light under different thermal conditions. We observe that the absorption coefficients shifted slightly from 50 nm to 61 nm when the system is applied by temperature. The nanocrystal shows the ability to absorb UV light and speedily declines throughout the 500 nm wavelength. The absorption peak observed is positioned at

approximately 75 nm of absorption value $40 \times 10^4 \text{ cm}^{-1}$. Figure 3(d) represents the electron energy loss spectrum $L(\omega)$. The highest peak of $L(\omega)$, which denotes the characteristic associated with plasma resonance, is observed at the plasma frequency of 23.2 eV and shifted to 19.7 eV when the respective temperature is given. Figure 3(e) shows the calculated reflectivity value for MgO without temperature effect at the zero frequency is 30% and decreases to 7% when the temperature is applied. (Figure 3(e)). The maximum reflectivity is noted at 22.8 eV, and 18.8 eV corresponds to 93.4 % and 99.8 % with and without temperature effect.



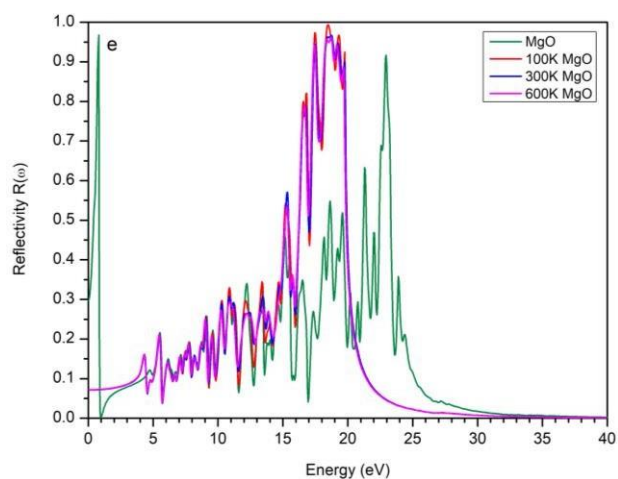


Figure 3: (a) Real part $\epsilon_1(\omega)$ (b) Imaginary part $\epsilon_2(\omega)$ (c) Absorption coefficient $\alpha(\omega)$ (d) Energy-loss spectrum $L(\omega)$, and (e) Reflectivity $R(\omega)$ for parallel field polarizations.

3.3 Electronic Properties

The band structure of the MgO crystal is presented in Figure 4(i). The bandgap of MgO at equilibrium state was calculated as an insulator with a wide direct bandgap value of 4.180 eV. Both the CBM and VBM are located at the same k-vector positions in the Brillouin zone. The electrons in the valence band are fully occupied due to the covalent bonds. They hence must achieve energy equal to the bandgap to move into the conduction band and achieve conductivity. The bandgap value obtained is considerably close to a previous theoretical study conducted using GGA of value 4.514 eV [18]. Based on Figures 4(ii) and (iii), we observe the temperature value of 100K and 300K does not affect the bandgap value much and only decreases slightly by 4.071 eV and 4.076 eV, respectively.

On the other hand, the bandgap decreases exceedingly for the 600K temperature of 3.876 eV, as shown in Figure 4(iii). We also note that the temperature applied might cause a change in the pattern of the band structure. However, it remains a direct bandgap at the G to G point. Figure 5 shows the total density of states (TDOS) MgO and partial density of states (PDOS) for Mg and O atoms separately. Mg 3p-orbital and O 2p-orbital mainly occupy the conduction band minimum and valence band maximum.

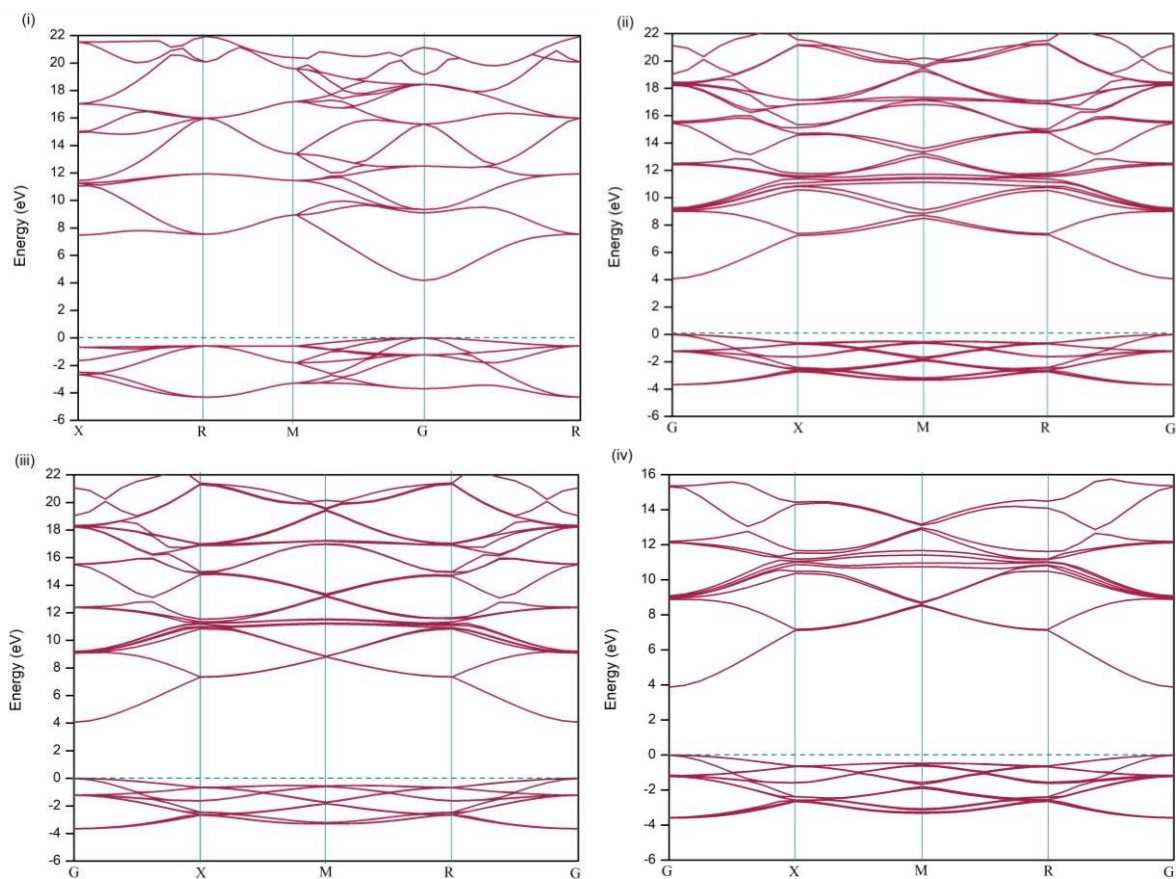


Figure 4: Calculated energy band structure of MgO at (i) 0K (ii) 100K (iii) at 300K and (iv) at 600K

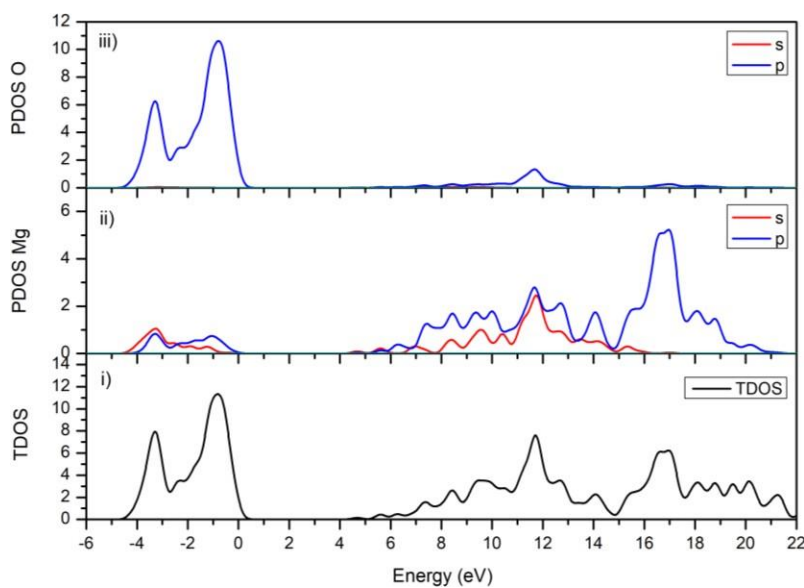


Figure 5: (i) Total Density of States (TDOS) of MgO (ii) Partial Density of States (PDOS) of Mg atom and (iii) Partial Density of States (PDOS) of O atom

4. Conclusion

In summary, the DFT study of MgO nanocrystal covers the electronic and optical properties of MgO by the generalized gradient approximation (GGA). The band structure of this material has a direct energy bandgap of about 4.180 eV. Our results show that the optical properties are affected by the inconsistent temperature manners despite the different temperatures given to the system. The absorption coefficient shows that MgO shows good coverage in the ultraviolet range. The bulk MgO is a direct bandgap nanocrystal at the G point in the Brillion Zone despite its temperature. The temperature is applied to alter the bandgap pattern and closes the bandgap at a high temperature. The PDOS and imaginary part of the dielectric function further confirm the insulator properties of the observed bandgap. Our absorption curve confirms that the nanocrystal is a good candidate for ultraviolet device application with a significantly high reflectivity percentage.

Conflicts of Interest

The authors declare no conflict of interest.

Acknowledgements

The author would like to acknowledge the Ionics Materials & Devices (iMADE) Research Laboratory, Institute of Science, UiTM Malaysia, for the facilities and support provided during the completion of this research.

References

- [1] J. Meyer, S. Hamwi, M. Kroger, W. Kowalsky, T. Riedl, A.Kahn, *Adv. Mater.* 2012; 24: 5408
- [2] Y.K. Mishra, G. Modi, V. Cretu, V. Postica, O. Lupan, T. Reimer, I. Paulowicz, V. Hrkac, W. Benecke, L. Kienle, R. Adelung, *Appl. Mater. Interfaces.* 2015; 7: 14303
- [3] Y.K. Mishra, S. Kaps, A. Schuchardt, I. Paulowicz, X. Jin, D. Gedamu, S. Wille, O. Lupan, R. Adelung, *Kona Powder Part J.* 2014; 31: 92.
- [4] O. Lupan, T. Braniste, M. Deng, L. Ghimpu, I. Paulowicz, Y.K. Mishra, L. Kienle, R. Adelung, I. Tiginyanu. *Sens. Actuator B-Chem.* 2015; 221: 544.
- [5] O. Lupan, V. Cretu, V. Postica, N. Ababii, O. Polonskyi, V. Kaidas, F. Schütt, Y.K. Mishra, E. Monaico, I. Tiginyanu, V. Sontea, T. Strunskus, F. Faupel, R. Adelung, *Sens. Actuator B-Chem.* 2016; 224: 434.

- [6] V. Cretu, V. Postica, A.K. Mishra, M. Hoppe, I. Tiginyanu, Y.K. Mishra, L. Chow, N.H. de Leeuw, R. Adelung, O. Lupan, *J. Mater. Chem. A*. 2016; 4: 6527
- [7] Neetu Singh, Prabhat Kumar Singh, Anuradha Shukla, Satyendra Singh, Poonam Tandon, *Journal of Inorganic and Organometallic Polymers and Materials*. 2016; 26: 1413–1420.
- [8] M.A. Fox, M. T. Dulay, *Chem. Rev.* 1993; 93: 341–357.
- [9] P. Pechy, T. Renouard, S.M. Zakeeruddin, S. R. Humphry-Baker, P. Comte, P. Liska, L.Cevey, E. Costa, V. Shklover, L. Spiccia, *J. Am. Chem. Soc.* 2001; 123: 1613–1624.
- [10] V.Piriyawong, V. Thongpool, P. Asanithi, & P. Limsuwan, *Journal of Nanomaterials*. 2012; 819403: 1–6.
- [11] M. Fernandez-Garcia, A. Martinez-Arias, J.C. Hanson, J.A. Rodriguez, *Chem. Rev.* 2004; 104; 4063
- [12] A. Bouhemadou, R. Khenata, *Comput. Mater. Sci.* 2007; 39: 803.
- [13] R. Saniz, L.H. Ye, T. Shishidou, J. Freeman. *Phys. Rev. B*. 2006; 74: 014209
- [14] L. Wang, T. Maxisch, G. Ceder. *Phys. Rev. B*. 2006; 73: 195107.
- [15] Nourozi, B., et al., *Results in Physics*.2019; 12: 2038-2043.
- [16] Wyckoff, R.W.G., *Crystal structures. Krieger*. 1964; 2.
- [17] Reddy, K.D., P. Kistaiah, and L. Iyengar, *Journal of the Less Common Metals*. 1983; 92: 81-84.
- [18] Singh, N., et al., *Journal of Inorganic Organometallic Polymers Materials*. 2016; 26; 1413- 1420.